RSC Advances

PAPER

View Article Online
View Journal | View Issue

Cite this: *RSC Adv.*, 2024, **14**, 7664

Novel sulfonamide derivatives as multitarget antidiabetic agents: design, synthesis, and biological evaluation†

Mohammed Salah Ayoup, *[ab] Nourhan Khaled,[a] Hamida Abdel-Hamid,[a] Doaa A. Ghareeb,[c] Samah A. Nasr,[c] Ahmed Omer,[de] Amr Sonousi,[fg] Asmaa E. Kassab *[f] and Abdelazeem S. Eltaweil[ah]

A series of new sulfonamide derivatives connected through an imine linker to five or seven membered heterocycles were designed and synthesized. All synthesized derivatives were characterized using a variety of spectroscopic methods, including IR, ^{1}HNMR, and ^{13}CNMR. *In vitro* α-glucosidase and α-amylase inhibition activities, as well as glucose uptake were assessed for each of the synthesized compounds. Four sulfonamide derivatives namely **3a**, **3b**, **3h** and **6** showed excellent inhibitory potential against α-glucosidase with IC_{50} values of 19.39, 25.12, 25.57 and 22.02 μM, respectively. They were 1.05- to 1.39-fold more potent than acarbose. Sulfonamide derivatives **3g**, **3i** and **7** (EC_{50} values of 1.29, 21.38 and 19.03 μM, respectively) exhibited significant glucose uptake activity that were 1.62- to 27-fold more potent than berberine. Both α-glucosidase protein (PDB: 2QMJ) and α-amylase (PDB: 1XCW) complexed with acarbose were adopted for docking investigations for the most active synthesized compounds. The docked compounds were able to inhabit the same space as the acarviosin ring of acarbose. The docking of the most active compounds showed an analogous binding with the active site of α-glucosidase as acarbose. The superior activity of the synthesized compounds against α-glucosidase enzyme than α-amylase enzyme can be rationalized by the weak interaction with the α-amylase. The physiochemical parameters of all synthesized compounds were aligned with Lipinski's rule of five.

Received 11th February 2024
Accepted 22nd February 2024

DOI: 10.1039/d4ra01060d

rsc.li/rsc-advances

1. Introduction

The pandemic of type 2 diabetes mellitus (T2DM) is a multifactorial chronic health condition and financial burden on modern society.[1] It accounts for 90% of all cases of diabetes,[2] being distinguished by persistent hyperglycemia brought on by the inability to utilize insulin due to a problem with the pancreatic β-cells.[3,4] More than 400 million people globally had T2DM in 2018. The number of diabetic people is increasing at an alarming rate, and by 2030, this figure is expected to increase to nearly 500 million.[5,6] In 2019,[7] diabetes mellitus was the cause of 4.2 million deaths worldwide. T2DM can lead to serious chronic consequences include end-stage renal disease, blindness, vascular disease, poor wound healing, and limb amputation. It also causes a number of dysfunctions in many organs and tissues.[8] Only a small percentage of patients with T2DM are able to maintain long-term glycemic control, despite the development of numerous therapy choices.[9,10] Controlling the elevated blood glucose levels is the primary treatment method for this disease. Retarding, controlling, and/or blocking carbohydrate hydrolytic enzymes are methods for regulating blood sugar levels.[11] Starch hydrolysis is facilitated by pancreatic enzymes such α-amylase and α-glucosidase, which elevates postprandial hyperglycemia. The key factor causing T2DM to develop is this rise in blood sugar levels. Therapeutically, this postprandial hyperglycemia is managed by blocking these enzymes that break down carbohydrates. The delay in glucose absorption caused by α-amylase and α-glucosidase inhibitors lowers blood sugar levels.[12,13] Many α-amylase and α-

[a]*Department of Chemistry, Faculty of Science, Alexandria University, Alexandria, Egypt. E-mail: mayoup@kfu.edu.sa; mohammedsalahayoup@gmail.com*
[b]*Department of Chemistry, College of Science, King Faisal University, Al-Ahsa 31982, Saudi Arabia*
[c]*Bio-screening and Preclinical Trial Lab, Biochemistry Department, Faculty of Science, Alexandria University, Alexandria, Egypt*
[d]*Polymer Institute of the Slovak Academy of Sciences, Dúbravská Cesta 9 845 41, Bratislava, Slovakia*
[e]*Polymer Materials Research Department, Advanced Technology and New Materials Research Institute (ATNMRI), City of Scientific Research and Technological Applications (SRTA-City), New Borg El-Arab City, Alexandria 21934, Egypt*
[f]*Department of Pharmaceutical Organic Chemistry, Faculty of Pharmacy, Cairo University, P.O. Box 11562 Kasr El-Aini Street, Cairo, Egypt. E-mail: asmaa.kassab@pharma.cu.edu.eg*
[g]*University of Hertfordshire hosted by Global Academic Foundation, New Administrative Capital, Cairo, Egypt*
[h]*Department of Engineering, Faculty of Technology and Engineering, University of Technology and Applied Sciences, Sultanate of Oman*

† Electronic supplementary information (ESI) available. See DOI: https://doi.org/10.1039/d4ra01060d

glucosidase inhibitors, including acarbose, miglitol, and voglibose, are utilized clinically to treat diabetic patients.[14,15] The other common groups of drugs for treating hyperglycemia are sulfonylureas (which enhance insulin release from pancreatic islets), biguanides (which decrease hepatic glucose synthesis), and peroxisome proliferator-activated receptor-γ (PPARγ) agonists (which increase insulin action).[16] These medications can be taken either on their own or in combination with other hypoglycemic treatments. Severe hypoglycemia, weight gain, decreased therapeutic efficiency as a result of an incorrect or ineffective dosing regimen, low potency and altered adverse effects as a result of drug metabolism, as well as problems with target specificity, solubility, and permeability are the main disadvantages of taking these conventional medications.[17] Another crucial tactic that can be used to control blood glucose levels and prevent diabetic hyperglycemia is the stimulation of glucose uptake from the bloodstream.[18,19] Most drug design efforts in recent years have focused on creating agents with a wide range of physiological effects, especially for diseases with complicated etiologies like diabetes. The development of these multi-target ligands must prioritize the choice of appropriate targets, which must be thoroughly characterized and are ideally linked to several disease-related pathways, as well as the optimization of the relative potency of the drug towards each receptor.[20] Drugs that target proteins in several biochemical pathways contributing to the pathogenesis of diabetes mellitus are necessary because of the pathological complexity of this disease. To improve patient compliance, research is also concentrating on identifying multi-targeted ligands.[21–23] Several researches described the synthesis of sulfonamides containing molecules that act as antidiabetics by inhibiting α-glucosidase enzyme.[24–30] These compounds contain some common structural features namely a *p*-substituted sulfonamide ring attached to a nitrogen-containing spacer which is consequently attached to phenyl, cyclic, or heterocyclic ring as in compounds **A**,[30] **B**[27] and **C**[28] (Fig. 1). The goal of our work is to synthesize new sulfonamide derivatives with the same essential pharmacophoric features of the reported compounds (Fig. 1). Firstly, a phenyl sulfonamide scaffold substituted at the *p*-position was used in the design of targeted compounds. The 2nd strategy involved the incorporation of a linker with imine imine-containing group. Both the phenyl sulfonamide motif and the linker were selected to share as H-bond acceptors and/or donors with amino acids in the active sites of α-glucosidase and α-amylase enzymes. Within the 3rd strategy, a five-membered heterocycle (pyrazole or oxazole) or seven-membered heterocycle (diazepine or triazepine ring featuring carbonyl or thioxo group) was grafted. The 4th strategy involved the introduction of variable hydrophobic aromatic moieties on the pyrazole motif. These hydrophobic moieties' substitution design was chosen to ensure a variety of electronic and lipophilic environments, which could affect the activity of the target compounds. In this study, all the synthesized compounds were evaluated for their *in vitro* α-glucosidase and α-amylase inhibition activities as well as on glucose uptake by yeast cells. Docking studies were done, for the most active synthesized compounds, on both α-glucosidase protein (PDB: 2QMJ) and α-amylase (PDB: 1XCW) complexed with acarbose.

2. Results and discussion

2.1. Chemistry

The novel functionalization protocol of the bacteriostatic antibiotic sulfanilamide (Scheme 1) was accomplished initially by diazotization using $NaNO_2$/HCl/AcOH protocol to form the diazonium salt **1**. Rapid coupling of **1** with pre-prepared active carbanion of ethyl acetoacetate at 0 °C afforded the corresponding hydrazone ethyl-3-oxo-2-(2-(4-sulfamoylphenyl)-hydrazineylidene) butanoate (**2**). The structure of **2** was confirmed by IR which showed the strong band at ν_{max} cm^{-1} 3342, 3250, and 3164 correspond to (NH_2, NH), and 1687 for conjugated (CO), moreover the ^{1}HNMR

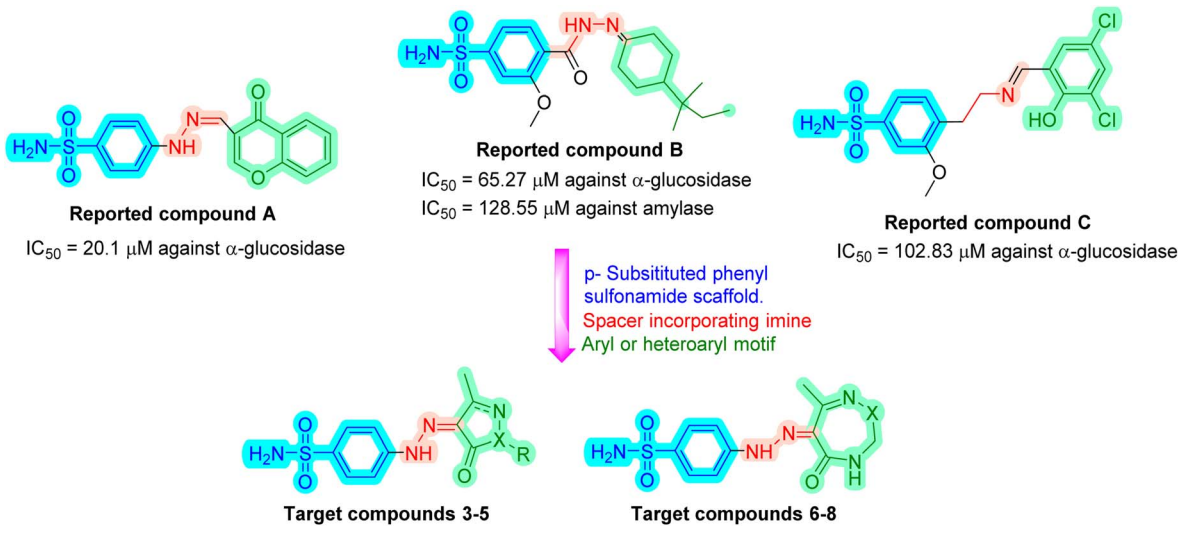

Fig. 1 Design strategy for the synthesized sulfonamide derivatives.

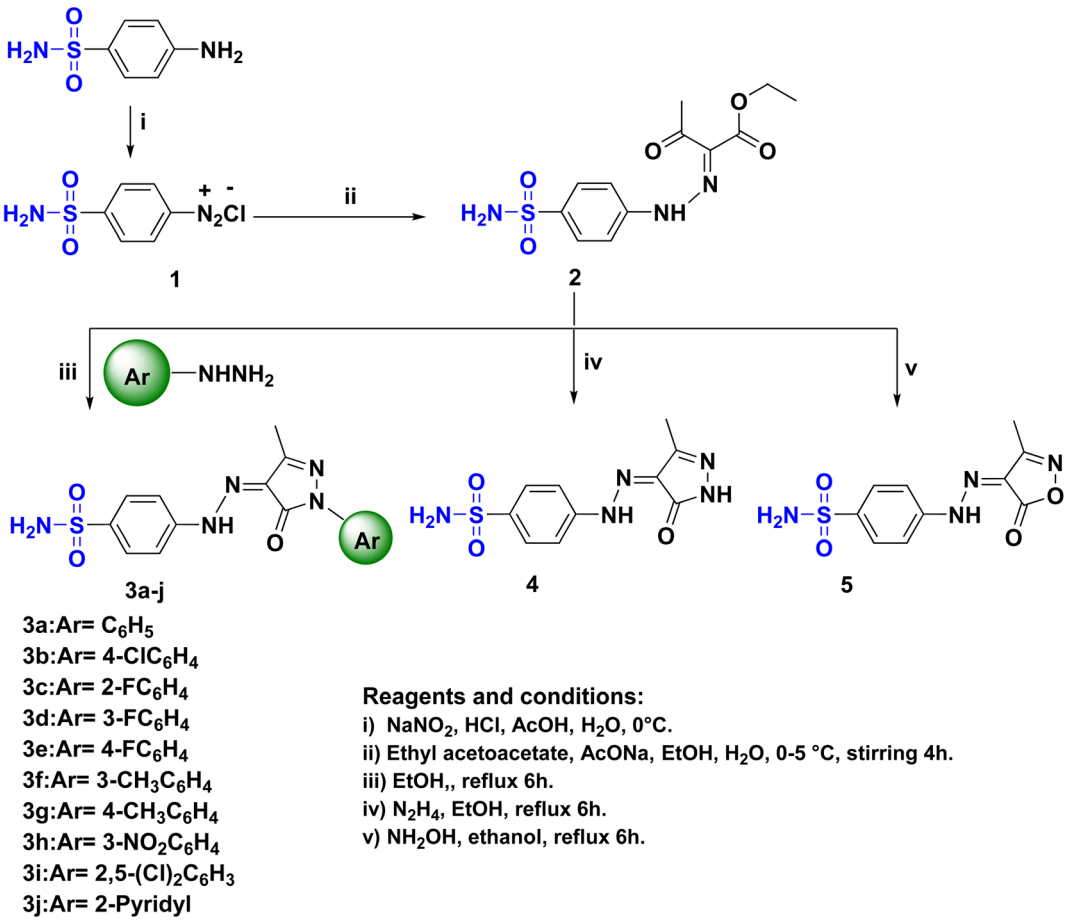

Scheme 1 The synthetic pathway and reagents for the preparation of the target compounds **1–5**.

spectrum of **2** showed two separate signals of NH and NH_2 at δ_H: 11.54 and 7.25 ppm, respectively. Also, three separated signals in the upfield at δ_H: 4.28, 2.37, and 1.24 ppm revealed the presence of OCH_2, $COCH_3$, and CH_3, respectively. Furthermore, the ^{13}CNMR spectrum confirmed the presence of the acetyl and ester groups where two nonhomotopic

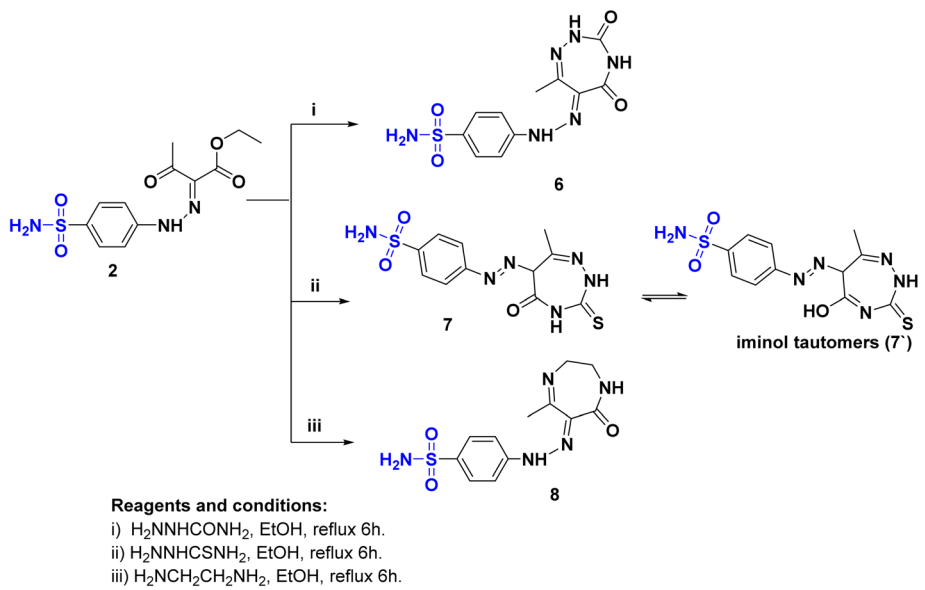

Scheme 2 The synthetic pathway and reagents for the preparation of the target compounds **6–8**.

Table 1 Biological evaluation results[a]

Compound	α-Glucosidase IC_{50}[b] (μM ± SD)	α-Amylase IC_{50}[b] (μM ± SD)	Glucose uptake EC_{50}[b] (μM ± SD)
3a	**19.39 ± 2.7**	416.46 ± 23.4	124.93 ± 9.8
3b	**25.12 ± 0.7**	267.19 ± 22.3	429.96 ± 33.1
3c	67.68 ± 7.1	219.29 ± 20.7	176.09 ± 11.8
3d	61.67 ± 5.6	225.55 ± 17.5	283.71 ± 19.5
3e	44.82 ± 3.4	237.41 ± 12.9	52.49 ± 4.9
3f	55.44 ± 4.8	249.10 ± 22.1	106.26 ± 9.8
3g	99.11 ± 6.8	73.93 ± 6.1	**1.29 ± 0.1**
3h	**25.57 ± 2.1**	152.23 ± 10.2	331.87 ± 22.9
3i	50.16 ± 4.8	137.95 ± 11.1	**21.38 ± 1.5**
3j	82.73 ± 7.4	293.86 ± 23.5	299.87 ± 15.9
4	76.04 ± 6.1	309.19 ± 25.1	101.39 ± 8.7
5	78.69 ± 5.9	75.72 ± 6.4	417.94 ± 22.5
6	**22.02 ± 1.9**	207.91 ± 10.8	235.27 ± 11.8
7	85.35 ± 2.3	331.96 ± 20.3	**19.03 ± 1.6**
8	109.81 ± 6.7	57.36 ± 4.2	277.79 ± 18.9
Acarbose	27.02 ± 1.6	13.14 ± 1.1	—
Berberine	—	—	34.70 ± 2.7

[a] The bold text indicates the compounds that are more potent than the reference standard. [b] All values are expressed as a mean of three replicates.

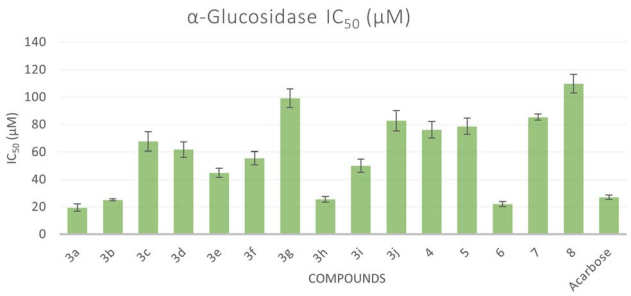

Fig. 2 Bar graph representation showing the comparative IC_{50} values for the α-glucosidase activity of the target compounds and acarbose as a reference drug.

carbonyls at δ_C: 194.4 and 162.8 ppm, respectively were present beside the aliphatic carbons at δ_C: 61.9, 25.8 and 14.3 ppm.

A series of sulfonamide hydrazone aryl pyrazole hybrids **3a–j** were prepared utilizing the hydrazone sulfonamide ethyl acetoacetate **2** by reflux in ethanol with arylhydrazines namely phenylhydrazine, *p*-chlorophenylhydrazine, *o*-fluorophenylhydrazine, *m*-fluorophenylhydrazine, *p*-fluorophenylhydrazine, *m*-methylphenylhydrazine, *p*-methylphenylhydrazine, *m*-nitrophenylhydrazine, 2,5-dichlorophenylhydrazine and 2-hydrazinopyridine (Scheme 1). The structure of the pyrazole hybrids were confirmed by NMR spectra where the ^{1}HNMR showed NH's at a range of δ_H: 13.19–13.03 ppm, the proton of SO_2NH_2 resonating at δ_H:7.34–7.36 ppm. The ^{13}CNMR of the hybrids **3a–j** showed carbonyl carbon at range δ_C: 157.0–156.7 ppm and the branched methyl group of pyrazole moiety at δ_C: 12.2–12.1 ppm. Moreover, the characteristic signal of the C–F bond of the aryl pyrazole **3c–e** appeared at δ_C: 157.3, 162.6, and 159.5 ppm, respectively with $^1J_{CF}$ = 240–249.5 Hz.[31,32] sulfanilamide hydrazone/pyrazole or isoxazole hybrids **4** and **5** (Scheme 1) were obtained by treatment of **2** with alcoholic hydrazine or hydroxyl amine, respectively. The IR spectra of **4** and **5** showed a split band revealed to NH_2 at ν_{max} 3208 and 3257 cm^{-1}, respectively. The ^{1}HNMR of **4** and **5** showed broad signals corresponding to NH at δ_H: 11.62 and 12.73 ppm, respectively beside the remarkable signals correspond to $\mathbf{H_2NSO_2}$ at δ_H: 7.32

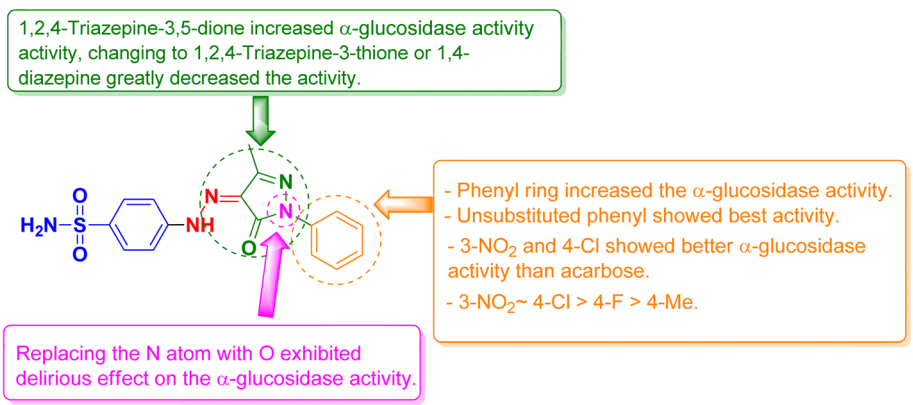

Fig. 3 Structure–activity relationship (SAR) of the synthesized sulfonamide derivatives.

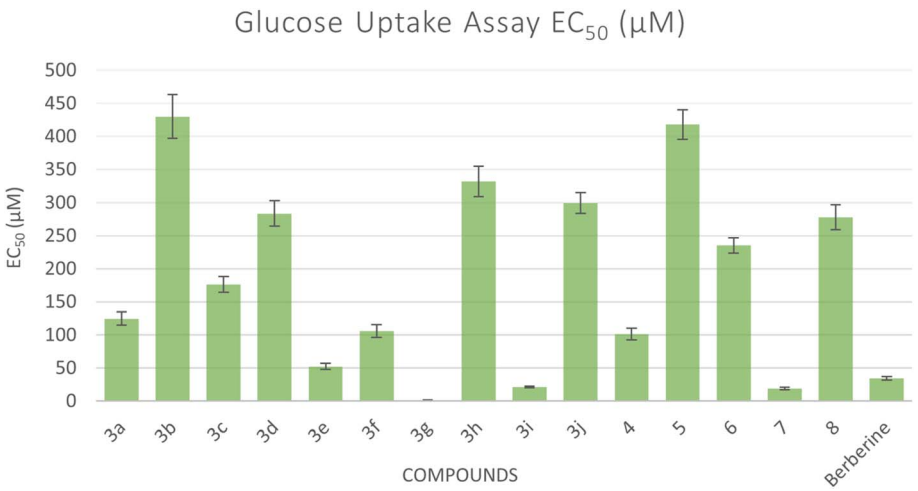

Fig. 4 Bar graph representation showing the comparative EC_{50} values for the glucose uptake activity of the target compounds and acarbose as a reference drug. EC_{50} means the concentration in μM of the compound that can cause 50% of glucose uptake by the yeast cells.

and 7.35 ppm, respectively. Moreover, the ^{13}CNMR confirmed the presence of C=O of the heterocyclic rings in compounds **4** and **5** which was indicated by a signal at δ_C: 160.4 and 160.6 ppm, respectively.

Novel sulfonamide hydrazone/seven-membered ring hybrids **6–8** (Scheme 2) were prepared by treatment of **2** with semicarbazide or thiosemicarbazide or ethylenediamine, respectively. The reaction proceeded through condensation followed by ring cyclization. The structures were confirmed by IR spectra, where a strong band in the range of 3307–3107 cm^{-1} revealed the presence of NH_2. The C=O band appeared at 1717–1680 cm^{-1}. The ^{1}HNMR confirmed the structure of compounds **6–8**, where **6** and **8** were present in the hydrazone form. While ^{1}HNMR of **6** showed four different signals correspond to four different nonhomototopic protons of three N–H′s at δ_H: 12.96, 7.55, and 7.23 ppm and SO_2NH_2 at δ_H: 7.35. Alternatively, hybrid **7** was present as in the azo form rather than hydrazono form in an equilibrium with a tautomer of the azo form **7′** as indicated from the ^{13}CNMR spectrum that revealed the presence of Csp^3-H at δ_C: 61.9 ppm corresponding to C6 of 1,2,4-triazepine moiety. Furthermore **8** is more flexible to exhibit tautomerism where the ^{13}C NMR represent the Csp3 at δ_C: 50.6, 38.6, 15.5 ppm.

2.2. α-Glucosidase inhibitory activity

All the synthesized compounds were evaluated for their *in vitro* α-glucosidase inhibition activities through the determination of their half maximal inhibitory concentration (IC_{50}) values compared to acarbose as a reference anti-diabetic drug. The results were summarized in Table 1 and represented graphically in Fig. 2. The results showed the most prominent sulfonamide derivatives namely **3a**, **3b**, **3h**, and **6** showed excellent inhibitory potential against α-glucosidase with IC_{50} values of 19.39, 25.12, 25.57, and 22.02 μM, respectively. In comparison to acarbose, they were 1.05 to 1.39 times more potent. Compounds **3c–f** and **3i** exhibited moderate α-glucosidase inhibitory activity with IC_{50}

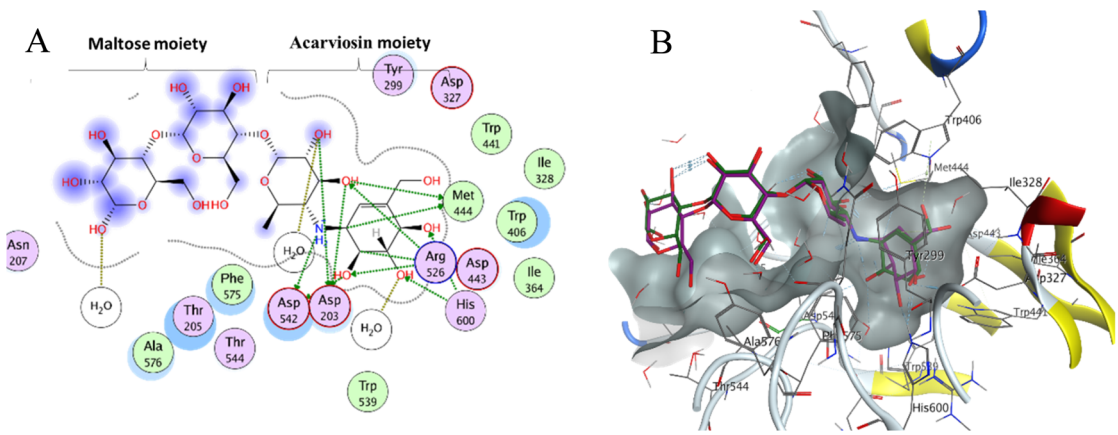

Fig. 5 (A) Two-dimensional diagram of acarbose binding with alpha-glucosidase binding pocket; (B) three-dimensional diagram of both the co-crystallized acarbose inhibitor (green) and its re-docked pose (magenta) in the active site of alpha-glucosidase showing RMSD (0.76 Å) within the acceptable range.

Table 2 The Lipinski parameters and the docking score of all target compounds

Compound	Docking score (PDB: 2QMJ) (kcal mol^{-1})	HBA (≤10)	HBD (≤5)	log *P* (−4.0–5)	PSA (0–150) $Å^2$	Interactions
3a	−6.054	5	2	3.495	117.22	HB (Asp327) HB (His600) Arene–H (Tyr299) Arene–H (Trp406)
3b	−6.295	5	2	4.087	117.22	HB (Asp327) HB (His600) Arene–H (Tyr299) Arene–H (Trp406)
3c	−6.394	5	2	2.364	117.22	HB (Asp327) HB (His600) HB (Asp443)
3d	−6.598	5	2	2.403	117.22	HB (Asp327) HB (His600)
3e	−6.385	5	2	3.648	117.22	HB (Asp327) HB (His600) HB (Asp443)
3f	−6.501	5	2	3.830	117.22	HB (Asp327) HB (His600) HB (Asp443)
3g	−6.212	5	2	3.793	117.22	HB (Asp327) HB (His600) HB (Asp443)
3h	−6.756	5	2	3.467	163.04	HB (Trp441) HB (Trp539) HB (Arg526) Arene–H (Tyr299) Arene–H (Phe575)
3i	−6.740	5	2	4.714	117.22	HB (Asp327) HB (His600) HB (Asp443)
3j	−6.193	6	2	2.668	130.11	HB (Asp327) HB (His600) HB (Asp443)
4	−5.644	5	3	1.644	126.01	HB (Asp203) HB (His600) HB (Met444) HB (Phe450) HB (Trp539) Arene–H (Tyr299) Arene–H (Trp406)
5	−5.516	5	2	2.112	123.21	HB (Met444) HB (Arg526) HB (Trp539) Arene–H (His600)
6	−5.695	6	4	1.265	155.11	HB (Asp327) HB (His600) HB (Asp443) Arene–H (Tyr299)
7	−5.694	6	4	3.216	170.13	HB (Asp327) HB (His600) HB (Asp443) Arene–H (Tyr299) Arene–H (Trp406)
8	−5.974	5	3	0.750	126.01	HB (Asp327) HB (His600) HB (Asp443) Arene–H (Tyr299)
Acarbose	−7.8552	18	13	−7.508	325.75	HB (Arg526) HB (Met444) HB (His600) HB (Asp203) HB (Asp542)

values in the range of 44.82 to 67.68 μM. Sulfonamide derivatives **3g**, **3j**, **4**, **5**, and **7** demonstrated weak α-glucosidase inhibitory potential with IC_{50} values in the range of 76.04 to 99.11 μM. Compound **8** (IC_{50} = 109.81 μM) showed the least inhibitory activity. The structure–activity relationship (SAR) was investigated. Unsubstituted phenyl ring as in compound **3a** showed the best α-glucosidase inhibitory activity. Substitutions on the phenyl ring generally decreased the activity but with 4-Cl (**3b**) and 3-NO_2 (**3h**) showed better activity than acarbose. Shifting of phenyl ring on the pyrazole scaffold to a hydrogen atom (**4**) or converting the pyrazole scaffold to isoxazole (**5**) by replacing the nitrogen atom with an oxygen atom exhibited a delirious effect on the α-glucosidase activity. 1,2,4-Triazepine-3,5-dione (**6**) increased α-glucosidase activity, changing to 1,2,4-triazepine-3-thione (**7**) or 1,4-diazepine (**8**) greatly decreased the activity (Fig. 3).

2.3. α-Amylase inhibitory activity

The inhibitory activities of all synthesized compounds against α-amylase were evaluated by calculating their half maximum inhibitory concentration (IC_{50}) values in comparison to acarbose, the standard anti-diabetic drug (Table 1). The results indicated that all the synthesized sulfonamide derivatives (IC_{50} values at the range of 57.36 to 416.46 μM) exhibited weak α-amylase inhibitory potential compared to acarbose.

2.4. Glucose uptake assay

The glucose uptake by the yeast cells [33]can be used as an *in vitro* screening tool to evaluate compounds for their hypoglycemic activity.[34] Glucose along with different concentrations of the tested compounds were added to yeast cells for a specific amount of time and the amount of glucose remained serves as an indication of the glucose uptake by the yeast cells. Five different concentrations were used for each compound and the EC_{50} values for all compounds were calculated which correspond to the concentration of the compound at which 50% of glucose uptake occurs. A lower EC_{50} shows a higher antidiabetic activity (Fig. 4). All compounds showed an increase in glucose uptake with increased concentrations (see ESI†). Compounds **3g**, **3i**, and **7** showed higher glucose uptake compared to berberine with EC_{50} of 1.29 μM, 21.38 μM, and 19.03 μM, respectively, representing 1.62- to 27-fold more potency than reference standard berberine (EC_{50} = 34.70 μM). However, other compounds demonstrated less glucose uptake activity compared to berberine.

2.5. Molecular docking study

Molecular docking is used as a computational method that can give valuable information about the binding interactions between the synthesized molecules and the active site of the target enzyme. This helps in evaluating the drugs and may propose further development. Docking studies were done, for the most active synthesized compounds, on both α-glucosidase protein (PDB: 2QMJ)[35] and α-amylase (PDB: 1XCW)[36] complexed with acarbose using MOE (2022.09)[37] software. The co-crystallized acarbose was docked first the active site to validate the docking protocol. The docking procedure was able to replicate the pose of acarbose with the relative mean standard deviation (RMSD) between the docked and the modeled acarbose within the cutoff limit (Fig. 5). The structure of acarbose consists of acarviosin moiety (2 rings) and maltose moiety (2 rings). In contrast to the maltose moiety that is solvent exposed and showed no binding with the enzyme, the acarviosin moiety is embedded deeply in the gorge of the active site and is responsible for its interaction with Arg526, Met444, His600, Asp203, Asp542 residues of the enzyme. The same docking protocol was then applied to the

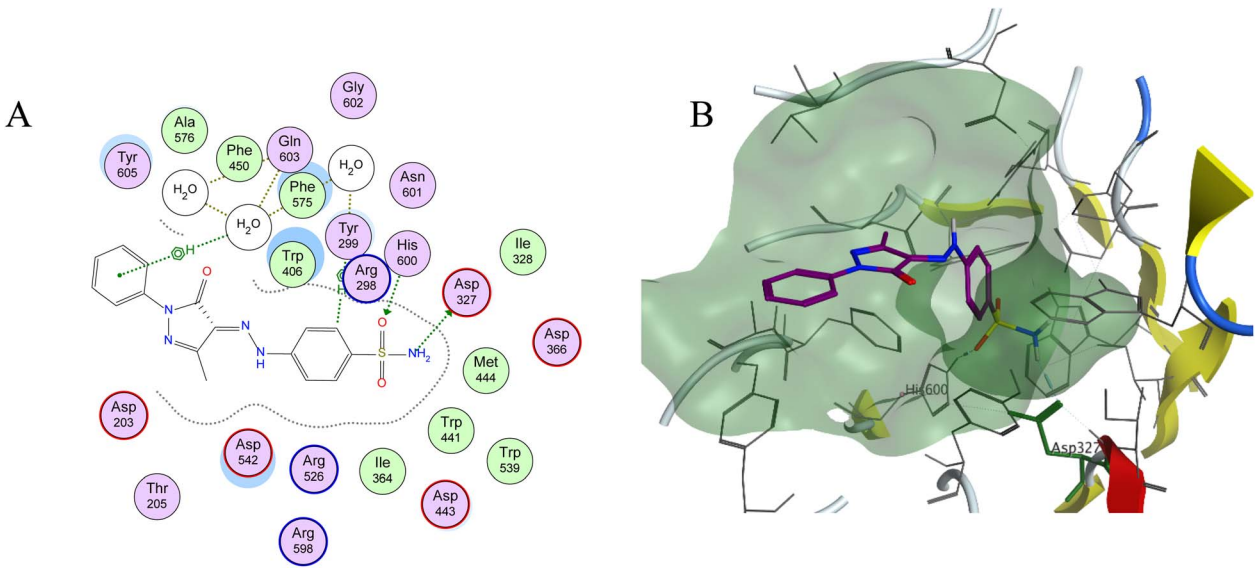

Fig. 6 (A) Two-dimensional diagram and (B) three-dimensional representation of molecular docking of compound **3a** (magenta) in the binding pocket (PDB: 2QMJ).

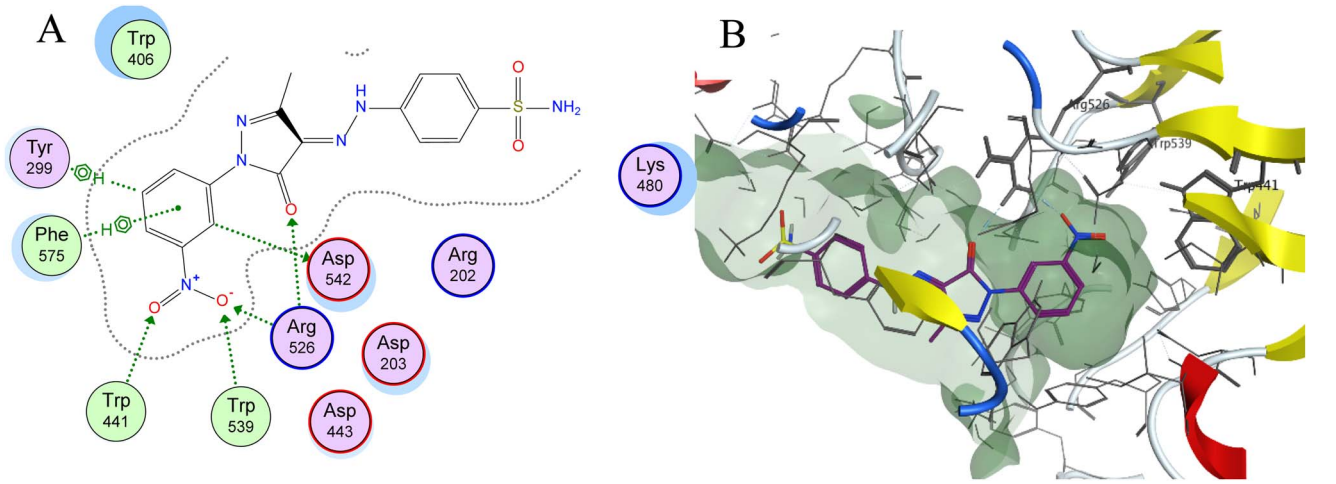

Fig. 7 (A) Two-dimensional diagram and (B) three-dimensional representation of molecular docking of compound **3h** (magenta) in the binding pocket (PDB: 2QMJ).

synthesized compounds to evaluate their interactions with the α-glucosidase binding site. The Lipinski parameters[38] and the docking results of the best derivatives along with the binding interactions are shown in Table 2. The physiochemical parameters of all synthesized compounds were aligned with Lipinski's rule of five. Generally, the docked compounds were able to inhabit the same region as the acarviosin ring of acarbose. The docking of the most active compounds (Fig. 6) showed an similar interaction with the active site as acarbose. The sulfonamide group of compounds **3a** was able to form hydrogen bond with His600 and Asp327. In addition, the phenyl ring interacts with Tyr299 and Trp406 *via* Arene–H interactions which help in the stabilization of the compound conformation in its active site. Compound **3h** with the *m*-nitro substitution showed higher interactions with the nitro group accepting 3 hydrogen bonds from Trp441, Trp539 and Arg526. Further, the pyrazolinone carbonyl oxygen bonded to Arg526 and the phenyl ring interacts with Tyr299 and Phe575 *via* Arene–H interactions (Fig. 7). In contrast, the docking simulation of the least active compounds **8** and **5** showed less binding energy to the active site (-5.974 kcal mol^{-1} and -5.516 kcal mol^{-1}, respectively) albeit the same binding pattern (docking poses of compounds are included in ESI†). The synthesized compounds demonstrated superior activity to α-glucosidase enzyme than α-amylase enzyme. For example, compound **3a** was 21 times more active towards α-glucosidase enzyme ($IC_{50} = 19.39$ μM) than α-amylase enzyme ($IC_{50} = 416.46$ μM). This difference in activity can be explained by the weak interaction with the α-amylase. The docking of compound **3a** in the active site of α-amylase (PDB: 1XCW) showed that compound **3a** has less binding interaction with the α-amylase with only one hydrogen bond with Glu233 (Fig. 8).

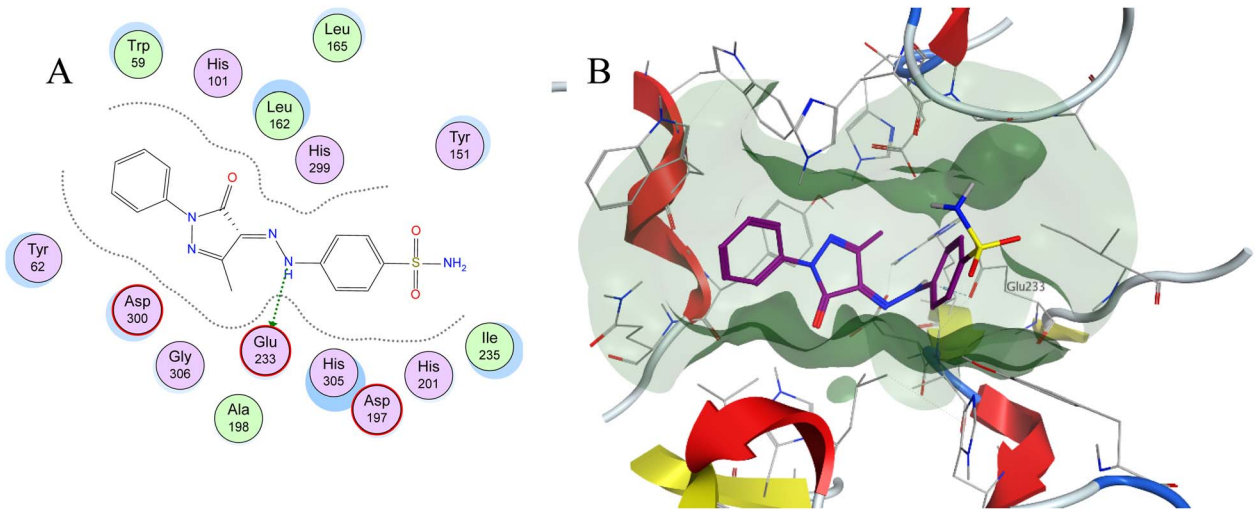

Fig. 8 (A) Two-dimensional diagram and (B) three-dimensional representation of molecular docking of compound **3a** (magenta) in the binding pocket (PDB: 1XCW).

3. Conclusion

In conclusion, a series of novel sulfonamides were synthesized and evaluated for their α-glucosidase, and α-amylase enzyme activity as well as their glucose uptake activity. Out of these fifteen novel compounds, four compounds showed better α-glucosidase inhibitory compared to the acarbose reference such as **3a** (19.39 μM for α-glucosidase), **3b** (25.12 μM for α-glucosidase), **3h** (25.57 μM for α-glucosidase) and **6** (22.02 μM for α-glucosidase). All compounds showed less α-amylase inhibition activity compared to acarbose. This low amylase activity can be rationalized computationally by the weak interactions of the compounds with the gorge of the α-amylase active site. Compounds **3g**, **3i**, and **7** showed better glucose uptake activity with EC_{50} compared to berberine (EC_{50} = 34.70 μM) values of 1.29, 21.38 and 19.03 μM, respectively.

4. Experimental

4.1. Chemistry

4.1.1. Procedure for the preparation of ethyl-3-oxo-2-(2-(4-sulfamoylphenyl)-hydrazineylidene)butanoate (2). A solution of sodium nitrite (1.5 mmol in 10 mL H_2O) was dropwisely added to solution of sulfanilamide (1.0 mmol) in AcOH (20 mL), HCl (6 M, 0.5 ml), and H_2O (5 mL) at 0 °C, the formed soluble diazonium salt solution was added to previously prepared solution from ethylacetoacetae (1.0 mmol) and AcONa (1.5 mmol) in ethanol (25 mL) and water (5.0 mL) at 0–5 °C the reaction mixture was kept to stir for 4 hours, the precipitated solid was filtered and recrystallized from ethanol to give **2** as yellow powder in 77% yield, m.p. 139–141 °C, R_f = 0.54 (EtOAc : *n*-hexane, 2 : 1); IR: ν_{max} cm^{-1} 3342, 3250 (NH_2), 3164 (NH), 2994 (Csp3-H), 1687 (CO); ^{1}H NMR (500 MHz, DMSO-d_6) δ_H:11.54 (s, 1H, N–H), 7.76 (d, J = 9.0 Hz, 2H, Ar–H), 7.50 (d, J = 9.0 Hz, 2H, Ar–H), 7.25 (s, 2H, NH_2SO_2), 4.28 (q, J = 7.5 Hz, 2H, OC**H**$_2$), 2.37 (s, 3H, C**H**$_3$), 1.24 (t, J = 7.0 Hz, 3H, CH_2C**H**$_3$), ^{13}C NMR (125 MHz, DMSO-d_6) δ_C: 194.4, 162.8, 145.7, 138.8, 133.9, 127.8, 115.3 (Ar–C), 61.9, 25.8, 14.3 (aliphatic-C). Anal. calcd for $C_{12}H_{15}N_3O_5S$ (313.07): C, 46.00; H, 4.83; N, 13.41. Found: C, 46.21; H, 5.04; N, 13.12.

4.1.2. General procedure for the preparation of compounds (3a–j). To a solution of **2** (0.32 mmol) in ethanol (10 mL), 0.32 mmol of arylhydrazine namely phenylhydrazine, *p*-chlorophenylhydrazine, *o*-fluorophenylhydrazine, *m*-fluorophenylhydrazine, *p*-fluorophenylhydrazine, *m*-methylphenylhydrazine, *p*-methylphenylhydrazine, *m*-nitrophenylhydrazine, 2,5-dichlorophenylhydrazine and 2-hydrazinopyridine was added, the reaction mixture was heated near boiling point for 6 hours, then the solid formed was filtered, and crystallized from ethanol to give:

*4.1.2.1. 4-(2-(3-Methyl-5-oxo-1-phenyl-1,5-dihydro-4H-pyrazol-4-ylidene) hydrazinyl)benzenesulfonamide (**3a**).* As reddish orange crystal; 72% yield; m.p. 260–263 °C; R_f = 0.62 (EtOAc : *n*-hexane, 2 : 1); IR: ν_{max} cm^{-1} 3350, 3327 (NH_2), 3249 (NH), 2924 (Csp3-H), 1668 (CO). ^{1}H NMR (500 MHz, DMSO-d_6) δ_H: 13.19 (s, 1H, N–H), 7.87 (d, J = 8.0 Hz, 2H, Ar–H), 7.83 (d, J = 8.5 Hz, 2H, Ar–H), 7.72 (d, J = 8.0 Hz, 2H, Ar–H), 7.42 (t, J = 7.5 Hz, 2H, Ar–H), 7.35 (s, 2H, **H**$_2$NSO$_2$), 7.18 (t, J = 8.0 Hz, 1H, Ar–H), 2.27 (s, 3H, C**H**$_3$). ^{13}C NMR (125 MHz, DMSO-d_6) δ_C: 156.7, 149.2, 144.5, 140.8, 138.3, 129.9, 129.6, 127.8, 125.4, 118.2, 116.6 (Ar–C), 12.1 (aliphatic-C). Anal. calcd for $C_{16}H_{15}N_5O_3S$ (357.09): C, 53.77; H, 4.23; N, 19.60. Found: C, 53.52; H, 4.34; N, 19.81.

*4.1.2.2. 4-(2-(1-(4-Chlorophenyl)-3-methyl-5-oxo-1,5-dihydro-4H-pyrazol-4-ylidene)hydrazinyl)benzenesulfonamide (**3b**).* Reddish orange crystal; 64% yield; m.p. = 247–249 °C; R_f = 0.51 (EtOAc : *n*-hexane, 1 : 1); IR: ν_{max} cm^{-1} 3339, 3250 (NH_2), 3104 (NH), 2992 (Csp3-H), 1654 (CO); ^{1}H NMR (500 MHz, DMSO-d_6) δ_H: 13.13 (s, 1H, N–H), 7.87 (d, J = 8.5 Hz, 2H, Ar–H), 7.82 (d, J = 8.5 Hz, 2H, Ar–H), 7.71 (d, J = 8.5 Hz, 2H, Ar–H), 7.46 (d, J = 8.5 Hz, 2H, Ar–H), 7.35 (s, 2H, N**H**$_2$SO$_2$), 2.24 (s, 3H, C**H**$_3$); ^{13}C NMR (125 MHz, DMSO-d_6) δ_C: 156.6, 149.6, 144.4, 140.9, 137.1, 129.6, 129.5, 129.1, 127.8, 119.5, 116.7 (Ar–C), 12.2 (aliphatic-C). Anal. calcd for $C_{16}H_{14}ClN_5O_3S$ (391.05): C, 49.05; H, 3.60; N, 17.87. Found: C, 49.31; H, 3.76; N, 17.96.

*4.1.2.3. 4-((2-(2-Fluorophenyl)-5-methyl-3-oxo-2,3-dihydro-1H-pyrazol-4-ylidene)hydrazinyl)benzenesulfonamide (**3c**).* As an orange powder; in 56% yield; m.p. 224–226 °C; R_f = 0.54 (EtOAc : *n*-hexane, 1 : 1); IR: ν_{max} cm^{-1} 3358, 3264 (NH_2), 3175 (NH), 2933 (Csp3-H), 1678 (CO); ^{1}H NMR (500 MHz, DMSO-d_6) δ_H: 13.08 (s, 1H, N–H), 7.82 (d, J = 9.5 Hz, 2H, Ar–H), 7.72 (d, J = 8.5 Hz, 2H, Ar–H), 7.50 (t, J = 7.5 Hz, 1H, Ar–H), 7.45–7.38 (m, 2H, Ar–H), 7.34 (s, 2H, **H**$_2$NSO$_2$), 7.29 (t, J = 7.5 Hz, 1H, Ar–H), 2.25 (s, 3H, C**H**$_3$); ^{13}C NMR (125 MHz, DMSO-d_6) δ_C: 157.3 (d, $^1J_{CF}$ = 249.5 Hz, **C**–F), 156.7, 149.4, 144.5, 140.8, 130.3 (d, $^3J_{CF}$ = 7.2 Hz, Ar–**C**), 128.9, 127.8 (d, $^2J_{CF}$ = 12 Hz), 125.4 (d, $^4J_{CF}$ = 2.5 Hz), 124.8 (d, $^2J_{CF}$ = 12 Hz, Ar–**C**), 117.2, 117.1, 116.7 (Ar–C) 12.2 (aliphatic-C). Anal. calcd for $C_{16}H_{14}FN_5O_3S$ (375.08): C, 51.20; H, 3.76; N, 18.66. Found: C, 51.43; H, 3.96; N, 18.85.

*4.1.2.4. 4-((2-(3-Fluorophenyl)-5-methyl-3-oxo-2,3-dihydro-1H-pyrazol-4-yl)-diazenyl)benzenesulfonamide (**3d**).* As yellowish orange powder; in 64% yield; m.p. 265–267 °C, R_f = 0.45 (EtOAc : *n*-hexane, 1 : 1); IR: ν_{max} cm^{-1} 3378, 3315 (NH_2), 3238 (NH), 1672 (CO); ^{1}H NMR (500 MHz, DMSO-d_6) δ_H: 13.12 (s, 1H, N–H), 7.82 (d, J = 8.5 Hz, 2H, Ar–H), 7.73–7.67 (m, 4H, Ar–H), 7.47–7.46 (m, 1H, Ar–H), 7.35 (s, 2H, **H**$_2$NSO$_2$), 7.0 (t, J = 7.0 Hz, 1H, Ar–H), 2.25 (s, 3H, C**H**$_3$); ^{13}C NMR (125 MHz, DMSO-d_6) δ_C: 162.6 (d, $^1J_{CF}$ = 240 Hz, **C**–F), 156.8, 149.8, 144.4, 140.9, 139.7 (d, $^3J_{CF}$ = 10.7, **C**F), 131.4 (d, $^4J_{CF}$ = 8.3, **C**F), 127.8, 116.7, 113.6, 111.8 (d, $^2J_{CF}$ = 21.5 Hz, **C**F), 104.8 (d, $^2J_{CF}$ = 27.5 Hz, **C**F) (Ar–C), 12.2 (aliphatic-C). Anal. calcd for $C_{16}H_{14}FN_5O_3S$ (375.08): C, 51.20; H, 3.76; N, 18.66. Found: C, 51.38; H, 3.64; N, 18.76.

*4.1.2.5. 4-(2-(1-(4-Fluorophenyl)-3-methyl-5-oxo-1,5-dihydro-4H-pyrazol-4-ylidene)hydrazinyl)benzenesulfonamide (**3e**).* As orange powder; in 59% yield; m.p. 277–279 °C; R_f = 0.66 (EtOAc : *n*-hexane, 1 : 1); IR: ν_{max} cm^{-1} 3359, 3324 (NH_2), 3247 (NH), 2925 (Csp3-H), 1666 (CO). ^{1}H NMR (500 MHz, DMSO-d_6) δ_H: 13.15 (s, 1H, N–H), 7.88–7.81 (m, 4H, Ar–H), 7.72 (d, J = 8.0 Hz, 2H, Ar–H), 7.35 (s, 2H, **H**$_2$NSO$_2$), 7.27 (t, J = 8.5 Hz, 2H, Ar–H), 2.25 (s, 3H, C**H**$_3$). ^{13}C NMR (125 MHz, DMSO-d_6) δ_C: 159.5 (d, $^1J_{CF}$ = 240 Hz, **C**-F), 156.7, 149.3, 144.4, 140.8, 134.7, 129.7, 127.8, 120.2 (d, $^3J_{CF}$ = 8.3 Hz, Ar–**C**), 116.7, 116.3 (d, $^2J_{CF}$ = 22.7 Hz, Ar–**C**), 117.2, 117.1, 116.7 (Ar–**C**) 12.2 (aliphatic-C).

Anal. calcd for $C_{16}H_{14}FN_5O_3S$ (375.08): C, 51.20; H, 3.76; N, 18.66. Found: C, 51.31; H, 3.85; N, 18.42.

*4.1.2.6. 4-(2-(3-Methyl-5-oxo-1-(m-tolyl)-1,5-dihydro-4H-pyrazol-4-ylidene)-hydrazinyl)benzenesulfonamide (**3f**).* As pale orange solid; in 69% yield; m.p. 242–245 °C; $R_f = 0.68$ (EtOAc : *n*-hexane, 1 : 1); IR: ν_{max} cm^{-1} 3319, 3227 (NH_2), 3122 (NH), 2925 (Csp3-H), 1645 (CO); ^{1}H NMR (500 MHz, DMSO-d_6) δ_H: 13.18 (s, 1H, N–H), 7.82 (d, $J = 8.5$ Hz, 2H, Ar–H), 7.70–7.66 (m, 4H, Ar–**H**), 7.35 (s, 2H, **H**$_2$NSO$_2$), 7.27 (t, $J = 7.5$ Hz, 1H, Ar–H), 6.98 (d, $J = 8.0$ Hz, 1H, Ar–**H**), 2.29 (s, 3H, C**H**$_3$), 2.23 (s, 3H, C**H**$_3$); ^{13}C NMR (125 MHz, DMSO-d_6) δ_C: 156.7, 149.1, 144.4, 140.7, 138.9, 138.2, 129.9, 129.3, 127.8, 126.0, 118.6, 116.5, 115.3 (Ar–C), 21.7, 12.1 (aliphatic-C). Anal. calcd for $C_{17}H_{17}N_5O_3S$ (371.11): C, 54.98; H, 4.61; N, 18.86. Found: C, 55.12; H, 4.81; N, 18.91.

*4.1.2.7. 4-(2-(3-Methyl-5-oxo-1-(p-tolyl)-1,5-dihydro-4H-pyrazol-4-ylidene)-hydrazinyl)benzenesulfonamide (**3g**).* As orange powder; in 70% yield; m.p. 272–275 °C; R_f = 0.65 (EtOAc : *n*-hexane, 1 : 1); IR: ν_{max} cm^{-1} 3331, 3246 (NH_2), 3088 (NH), 2921 (Csp3-H), 1653 (CO)·^{1}H NMR (500 MHz, DMSO-d_6) δ_H: 13.18 (s, 1H, N–**H**), 7.82 (d, $J = 8.5$ Hz, 2H, Ar–**H**), 7.74–7.71 (m, 4H, Ar–**H**), 7.35 (s, 2H, **H**$_2$NSO$_2$), 7.21 (d, $J = 8.0$ Hz, 2H, Ar–**H**), 2.26 (s, 3H, C**H**$_3$), 2.24 (s, 3H, C**H**$_3$);^{13}C NMR (125 MHz, DMSO-d_6) δ_C: 156.5, 149.0, 144.4, 140.7, 135.9, 134.6, 129.9, 127.8, 118.2, 116.5 (Ar–C), 21.0, 12.1 (aliphatic-C). Anal. calcd for $C_{17}H_{17}N_5O_3S$ (371.11): C, 54.98; H, 4.61; N, 18.86. Found: C, 55.08; H, 4.77; N, 18.72.

*4.1.2.8. 4-(2-(3-Methyl-1-(3-nitrophenyl)-5-oxo-1,5-dihydro-4H-pyrazol-4-ylidene)hydrazinyl)benzenesulfonamide (**3h**).* As orange crystals; in 74% yield; m.p. 278–280 °C; R_f = 0.55 (EtOAc : *n*-hexane, 1 : 1); IR: ν_{max} cm^{-1} 3381 (NH), 3192, 3114 (NH_2), 1673 (CO); ^{1}H NMR (500 MHz, DMSO-d_6) δ_H: 13.09 (s, 1H, N–**H**), 8.74 (s, 1H, Ar–**H**), 8.22 (d, $J = 6.0$ Hz, 1H, Ar–**H**), 7.98 (d, $J = 6.5$ Hz, 2H, Ar–**H**), 7.98–7.68 (m, 6H, Ar–**H**), 7.36 (s, 2H, **H**$_2$NSO$_2$), 2.26 (s, 3H, C**H**$_3$); ^{13}C NMR (125 MHz, DMSO-d_6) δ_C: 156.8, 150.3, 148.5, 144.5, 141.0, 139.0, 131.2, 129.2, 127.8, 123.4, 119.5, 116.9, 111.7 (Ar–C), 12.2 (aliphatic-C). Anal. calcd for $C_{16}H_{14}N_6O_5S$ (402.07): C, 47.76; H, 3.51; N, 20.89. Found: C, 47.52; H, 3.74; N, 20.72.

*4.1.2.9. 4-(2-(1-(2,5-Dichlorophenyl)-3-methyl-5-oxo-1,5-dihydro-4H-pyrazol-4-ylidene)hydrazinyl)benzenesulfonamide (**3i**).* As a yellowish Orange powder; in 76% yield; m.p. 227–229 °C; R_f = 0.63 (EtOAc : *n*-hexane, 1 : 1); IR: ν_{max} cm^{-1} 3239 (NH), 3134, 3088 (NH_2), 1674 (CO). ^{1}H NMR (500 MHz, DMSO-d_6) δ_H: 13.03 (s, 1H, N–**H**), 7.82 (d, $J = 8.5$ Hz, 2H, Ar–**H**), 7.74 (d, $J = 8.5$ Hz, 2H, Ar–**H**), 7.66 (m, 2H, Ar–**H**), 7.54 (dd, $J = 8.5$, 2.0 Hz, 1H, Ar–**H**), 7.34 (s, 2H, **H**$_2$NSO$_2$), 2.25 (s, 3H, C**H**$_3$)·^{13}C NMR (125 MHz, DMSO-d_6) δ_C: 156.8, 149.4, 140.8, 136.0, 132.4, 132.1, 130.5, 130.0, 129.5, 128.6, 127.8, 116.8 (Ar–C), 12.2 (aliphatic-C). Anal. calcd for $C_{16}H_{13}Cl_2N_5O_3S$ (425.01): C, 45.08; H, 3.07; N, 16.43. Found: C, 45.22; H, 3.14; N, 16.51.

*4.1.2.10. 4-(2-(3-Methyl-5-oxo-1-(pyridin-2-yl)-1,5-dihydro-4H-pyrazol-4-ylidene)hydrazinyl)benzenesulfonamide (**3j**).* As an orange powder, in 70% yield; m.p. 274–276 °C, R_f = 0.69 (EtOAc : *n*-hexane, 2 : 1); IR: ν_{max} cm^{-1} 3294, 3227 (NH_2), 3109 (NH), 1723 (CO). ^{1}H NMR (500 MHz, DMSO-d_6) δ_H: 13.14 (s, 1H, N–**H**), 8.44 (s, 1H, Ar–H), 7.90–7.71 (m, 6H, Ar–**H**), 7.35 (s, 2H, **H**$_2$NSO$_2$), 7.24 (t, $J = 6.0$ Hz, 1H, Ar–**H**), 2.27 (s, 3H, C**H**$_3$). ^{13}C NMR (125 MHz, DMSO-d_6) δ_C: 157.0, 149.9, 149.4, 148.9, 144.6, 140.7, 138.9, 129.5, 127.8, 121.7, 116.7, 114.4 (Ar–C), 12.2 (aliphatic-C). Anal. calcd for $C_{15}H_{14}N_6O_3S$ (358.08): C, 50.27; H, 3.94; N, 23.45. Found: C, 50.03; H, 4.17; N, 23.22.

4.1.3. Procedure for the preparation of compounds 4 and 5. To a solution of **2** (0.32 mmol in ethanol 10 mL), (0.45 mmol) of NH_2NH_2 or NH_2OH respectively was added, the reaction mixture was heated near boiling point for 6 hours, then the solid formed was filtered, crystallized from ethanol to give **4** or **5** respectively.

*4.1.3.1. 4-(2-(3-Methyl-5-oxo-1,5-dihydro-4H-pyrazol-4-ylidene)hydrazinyl)-benzenesulfonamide (**4**).* As reddish orange powder; in 58% yield; m.p. 227–229 °C; R_f = 0.58 (EtOAc : *n*-hexane, 2 : 1); IR: ν_{max} cm^{-1} 3208 (split band, NH_2), 1677 (CO). ^{1}H NMR (500 MHz, DMSO-d_6) δ_H: 13.12 (bs, 1H, N–**H**), 11.62 (s, 1H, N–**H**), 7.79 (d, $J = 9.0$ Hz, 2H, Ar–**H**), 7.63 (d, $J = 9.0$ Hz, 2H, Ar–**H**), 7.32 (s, 2H, **H**$_2$NSO$_2$), 2.12 (s, 3H, C**H**$_3$)·^{13}C NMR (125 MHz, DMSO-d_6) δ_C: 160.4, 147.5, 144.6, 140.2, 130.2, 127.8, 116.0 (Ar–**C**), 12.1 (**C**H$_3$). Anal. calcd for $C_{10}H_{11}N_5O_3S$ (281.06): C, 42.70; H, 3.94; N, 24.90. Found: C, 42.54; H, 4.12; N, 24.81.

*4.1.3.2. 4-(2-(3-Methyl-5-oxoisoxazol-4(5H)-ylidene) hydrazinyl)benzene-sulfonamide (**5**).* As pale yellow powder, in 54% yield; m.p. 227–229 °C; R_f = 0.52 (EtOAc : *n*-hexane, 2 : 1); IR: ν_{max} cm^{-1} 3437 (split band, NH_2), 3257 (NH), 1720 (CO); ^{1}H NMR (500 MHz, DMSO-d_6) δ_H: 12.73 (s, 1H, N–**H**), 7.81 (d, J = 8.5 Hz, 2H, Ar–**H**), 7.76 (d, $J = 9.0$ Hz, 2H, Ar–**H**), 7.35 (s, 2H, **H**$_2$NSO$_2$), 2.22 (s, 3H, C**H**$_3$); ^{13}C NMR (125 MHz, DMSO-d_6) δ_C: 162.4, 160.6, 144.5, 141.2, 127.7, 122.7, 117.3 (Ar–C), 10.6 (aliphatic-C). Anal. calcd for $C_{10}H_{10}N_4O_4S$ (282.04): C, 42.55; H, 3.57; N, 19.85. Found: C, 42.71; H, 3.62; N, 19.72.

4.1.4. Procedure for the preparation of compounds 6–8. To a solution of **2** (0.32 mmol) in ethanol (10 mL), 0.35 mmol of semicarbazide, thiosemicarbazide or ethylenediamine was added respectively, the reaction mixture was heated near boiling point for 6 hours, then the solid formed was filtered, and crystallized from ethanol to give:

*4.1.4.1. 4-(2-(5-Methyl-3,7-dioxo-1,2,3,7-tetrahydro-6H-1,2,4-triazepin-6-ylidene)hydrazinyl)benzenesulfonamide (**6**).* As pale yellow powder, in 51% yield; m.p. 244–247 °C, $R_f = 0.56$ (EtOAc : *n*-hexane, 2 : 1); IR: ν_{max} cm^{-1} 3419 (NH), 3334, 3307 (NH_2), 3193 (NH), 2930 (Csp3-H), 1717 (CO); ^{1}H NMR (500 MHz, DMSO-d_6) δ_H: 12.96 (s, 1H, N–**H**), 7.82 (d, $J = 7.0$ Hz, 2H, Ar–**H**), 7.73 (d, J = 7.0 Hz, 2H, Ar–**H**), 7.55 (s, 1H, N–**H**), 7.35 (s, 2H, **H**$_2$NSO$_2$), 7.23 (s, 1H, N–**H**), 2.20 (s, 3H, C**H**$_3$); ^{13}C NMR (125 MHz, DMSO-d_6) δ_C: 157.8, 149.8, 149.5, 144.5, 141.0, 128.7, 127.8, 116.9, (Ar–C), 12.2 (aliphatic-C). Anal. calcd for $C_{11}H_{12}N_6O_4S$ (324.06): C, 40.74; H, 3.73; N, 25.91. Found: C, 40.85; H, 3.81; N, 25.71.

4.1.4.2. (E)-4-((7-methyl-5-oxo-3-thioxo-3,4,5,6-tetrahydro-2H-1,2,4-triazepin-6-yl)diazenyl)benzenesulfonamide (7). As yellowish green powder, in 58% yield; m.p. 233–235 °C, $R_f = 0.71$ (EtOAc : *n*-hexane, 2 : 1); IR: ν_{max} cm^{-1} 3431 (NH), 3244, 3207 (NH_2), 1682 (CO); ^{1}H NMR (500 MHz, DMSO-d_6) δ_H: 9.44 (s, 0.44H, N–**H**), 8.89 (s, 0.36H, N–**H**), 8.61 (m, 6H (Ar–H), (N**H**$_2$SO$_2$)), C**H**$_3$ appeared at 2.37 and 2.23; ^{13}C NMR (125 MHz, DMSO-d_6) δ_C: 181.6, 141.1, 127.8, 127.7, 117.2, 115.3 (Ar–C) 61.9, 14.1, 12.2 (aliphatic-C). Anal. calcd for $C_{11}H_{12}N_6O_3S_2$. (340.04) C, 38.82; H, 3.55; N, 24.69. Found: C, 38.95; H, 3.62; N, 24.87.

*4.1.4.3. 4-(2-(5-Methyl-7-oxo-1,2,3,7-tetrahydro-6H-1,4-diazepin-6-ylidene)hydrazinyl)benzenesulfonamide (**8**).* As a pale-yellow powder, in 60% yield; m.p. 283–285 °C; R_f = 0.67 (EtOAc : *n*-hexane, 2 : 1); IR: ν_{max} cm^{-1} broad peak 3312–3103 (OH, NH, and NH_2), 2945 (Csp3-H), 1638 (CO); ^{1}H NMR (500 MHz, DMSO-d_6) δ_H: 13.90 (s, 1H, N–**H**), 11.30 (s, 1H, N–**H**), 7.74–7.34 (m, 6H, Ar–**H**, $\mathbf{H_2}NSO_2$), 3.72–3.54 (m, 4H, $C\mathbf{H_2}C\mathbf{H_2}$), 2.20 (s, 3H, $C\mathbf{H_3}$); ^{13}C NMR (125 MHz, DMSO-d_6) δ_C: 168.8, 164.3, 145.9, 138.0, 130.1, 127.9, 114.4 (Ar–C), 50.6, 38.6, 15.5 (aliphatic-C). Anal. calcd for $C_{12}H_{15}N_5O_3S$ (309.09): C, 46.59; H, 4.89; N, 22.64. Found: C, 46.45; H, 4.81; N, 22.44.

4.2. Molecular modeling studies

The X-ray structure of the α-glucosidase enzyme (PDB: 2QMJ) and α-amylase (PDB: 1XCW) were downloaded from the protein databank (PDB) website (**https://www.rcsb.org/**), at a resolution of 1.90 Å and 2.00 Å respectively. All the molecular modeling and docking studies were carried out using MOE 2020.09 (Chemical Computing Group, Canada) as the computational software. First, all the hydrogen atoms were added using the Protonate 3D algorithm where the protonation states of the amino acid residues were assigned, and the partial charges of atoms were added. In addition, the compounds were drawn using the builder tool and energy was minimized using the MMFF94× force field. MOE induced-fit Dock tool used to dock the synthesized compounds into the active site. The selection of the final docked ligand–enzyme poses was according to the criteria of binding energy score and combined with ligand–receptor interactions.

4.3. Biological evaluation

The biological assays were carried out according to the previously reported procedures and have been provided in the ESI;† alpha-glucosidase inhibitory assay,[39] alpha-amylase inhibitory assay,[40] and glucose uptake assay.[33]

Conflicts of interest

The authors have no conflict of interest concerning this work.

Acknowledgements

Nourhan Khaled (M. Sc. Student, faculty of science, Alexandria University), a Scholarship student of Scientists for next generation (SNG) scholarship program (Call 8), N. K. would like to thank the Academy of Scientific Research and Technology, Cairo, Egypt for their financial contribution to this research.

References

1 M. H. Tschöp, B. Finan, C. Clemmensen, *et al.*, Unimolecular Polypharmacy for Treatment of Diabetes and Obesity, *Cell Metab.*, 2016, **24**(1), 51–62, DOI: **10.1016/j.cmet.2016.06.021**.
2 M. Laakso and J. Kuusisto, Insulin resistance and hyperglycaemia in cardiovascular disease development, *Nat. Rev. Endocrinol.*, 2014, **10**(5), 293–302, DOI: **10.1038/nrendo.2014.29**.
3 H. Kolb and D. L. Eizirik, Resistance to type 2 diabetes mellitus: a matter of hormesis?, *Nat. Rev. Endocrinol.*, 2012, **8**(3), 183–192, DOI: **10.1038/nrendo.2011.158**.
4 S. E. Kahn, M. E. Cooper and S. Del Prato, Pathophysiology and treatment of type 2 diabetes: perspectives on the past, present, and future, *Lancet*, 2014, **383**(9922), 1068–1083, DOI: **10.1016/S0140-6736(13)62154-6**.
5 S. Wild, G. Roglic, A. Green, R. Sicree and H. King, Global Prevalence of Diabetes, *Diabetes Care*, 2004, **27**(5), 1047–1053, DOI: **10.2337/diacare.27.5.1047**.
6 S. Basu, J. S. Yudkin, S. Kehlenbrink, *et al.*, Estimation of global insulin use for type 2 diabetes, 2018–30: a microsimulation analysis, *Lancet Diabetes Endocrinol.*, 2019, **7**(1), 25–33, DOI: **10.1016/S2213-8587(18)30303-6**.
7 I. D. Federation, *IDF Diabetes Atlas*, 9th edn, 2019.
8 Y. Lin and Z. Sun, Current views on type 2 diabetes, *J. Endocrinol.*, 2010, **204**(1), 1–11, DOI: **10.1677/JOE-09-0260**.
9 J. S. Skyler, Diabetes Mellitus: Pathogenesis and Treatment Strategies, *J. Med. Chem.*, 2004, **47**(17), 4113–4117, DOI: **10.1021/jm0306273**.
10 B. Ahrén, Islet G protein-coupled receptors as potential targets for treatment of type 2 diabetes, *Nat. Rev. Drug Discovery*, 2009, **8**(5), 369–385, DOI: **10.1038/nrd2782**.
11 J. B. Xiao and P. Hogger, Dietary polyphenols and type 2 diabetes: current insights and future perspectives, *Curr. Med. Chem.*, 2015, **22**(1), 23–38, DOI: **10.2174/09298673216614070613080 7**.
12 H. Laoufi, N. Benariba, S. Adjdir and R. Djaziri, In vitro α-amylase and α-glucosidase inhibitory activity of Ononis angustissima extracts, *J. Appl. Pharm. Sci.*, 2017, **7**(2), 191–198, DOI: **10.7324/JAPS.2017.70227**.
13 P. Agarwal and R. Gupta, Alpha-amylase inhibition can treat diabetes mellitus, *Res. Rev.: J. Med. Health Sci.*, 2016, **5**(4), 1–8.
14 M. TOELLER, α-Glucosidase inhibitors in diabetes: efficacy in NIDDM subjects, *Eur. J. Clin. Invest.*, 2010, **24**(S3), 31–35, DOI: **10.1111/j.1365-2362.1994.tb02253.x**.
15 H. Bischoff, Pharmacology of alpha-glucosidase inhibition, *Eur. J. Clin. Invest.*, 1994, **24**, 3–10.
16 A. Chaudhury, C. Duvoor, V. S. Reddy Dendi, *et al.*, Clinical review of antidiabetic drugs: implications for type 2 diabetes mellitus management, *Front. Endocrinol.*, 2017, **8**, 6, DOI: **10.3389/fendo.2017.0006**.
17 K. R. Feingold, B. Anawalt, A. Boyce, *et al.*, *Oral and Injectable (Non-insulin) Pharmacological Agents for Type 2 Diabetes*, Endotext South Dartmouth, MA, 2020.
18 Y. Zheng, S. H. Ley and F. B. Hu, Global aetiology and epidemiology of type 2 diabetes mellitus and its complications, *Nat. Rev. Endocrinol.*, 2018, **14**(2), 88–98, DOI: **10.1038/nrendo.2017.151**.
19 C. Hu and W. Jia, Therapeutic medications against diabetes: what we have and what we expect, *Adv. Drug Delivery Rev.*, 2019, **139**, 3–15, DOI: **10.1016/j.addr.2018.11.008**.

20 A. Artasensi, A. Pedretti, G. Vistoli and L. Fumagalli, Type 2 diabetes mellitus: A review of multi-target drugs, *Molecules*, 2020, **25**(8), 1–20, DOI: 10.3390/molecules25081987.

21 R. Ottanà, R. Maccari, M. Giglio, *et al.*, Identification of 5-arylidene-4-thiazolidinone derivatives endowed with dual activity as aldose reductase inhibitors and antioxidant agents for the treatment of diabetic complications, *Eur. J. Med. Chem.*, 2011, **46**(7), 2797–2806, DOI: 10.1016/j.ejmech.2011.03.068.

22 R. Ottanà, P. Paoli, M. Cappiello, *et al.*, Search for Multi-Target Ligands as Potential Agents for Diabetes Mellitus and Its Complications—A Structure-Activity Relationship Study on Inhibitors of Aldose Reductase and Protein Tyrosine Phosphatase 1B, *Molecules*, 2021, **26**(2), 330, DOI: 10.3390/molecules26020330.

23 M. Stefek, V. Snirc, P.-O. Djoubissie, *et al.*, Carboxymethylated pyridoindole antioxidants as aldose reductase inhibitors: Synthesis, activity, partitioning, and molecular modeling, *Bioorg. Med. Chem.*, 2008, **16**(9), 4908–4920, DOI: 10.1016/j.bmc.2008.03.039.

24 H. Ullah, M. Waseem, F. Rahim, A. Hussain and M. Perviaz, molecular docking study of oxadiazole-sulphonamide hybrid analogues, *Chem. Data Collect.*, 2023, **45**, 1–12.

25 F. A. Saddique, M. Ahmad, U. A. Ashfaq, M. Muddassar, S. Sultan and M. E. A. Zaki, Identification of Cyclic Sulfonamides with an N-Arylacetamide Group as α-Glucosidase and α-Amylase Inhibitors: Biological Evaluation and Molecular Modeling, *Pharmaceuticals*, 2022, **15**(1), 1–22, DOI: 10.3390/ph15010106.

26 L. Rasheed, W. Rehman, F. Rahim, *et al.*, Molecular Modeling and Synthesis of Indoline-2,3-dione-Based Benzene Sulfonamide Derivatives and Their Inhibitory Activity against α-Glucosidase and α-Amylase Enzymes, *ACS Omega*, 2023, **8**(17), 15660–15672, DOI: 10.1021/acsomega.3c01130.

27 Ç. B. Apaydın, G. Hasbal Çelikok, T. Yılmaz Özden and G. Cihan Üstündağ, Design, synthesis and biological evaluation of novel sulfonamide hydrazones as α-glucosidase and α-amylase inhibitors, *İstanbul J Pharm*, 2022, **52**(2), 108–113, DOI: 10.26650/istanbuljpharm.2022.1018698.

28 P. Taslimi, M. Işık, F. Türkan, *et al.*, Benzenesulfonamide derivatives as potent acetylcholinesterase, α-glycosidase, and glutathione S-transferase inhibitors: biological evaluation and molecular docking studies, *J. Biomol. Struct. Dyn.*, 2020, 1–12, DOI: 10.1080/07391102.2020.1790422.

29 M. Askarzadeh, H. Azizian, M. Adib, *et al.*, Design, synthesis, in vitro α-glucosidase inhibition, docking, and molecular dynamics of new phthalimide-benzenesulfonamide hybrids for targeting type 2 diabetes, *Sci. Rep.*, 2022, **12**(1), 1–16, DOI: 10.1038/s41598-022-14896-2.

30 G. Wang, M. Chen, J. Wang, *et al.*, Synthesis, biological evaluation and molecular docking studies of chromone hydrazone derivatives as α-glucosidase inhibitors, *Bioorg. Med. Chem. Lett.*, 2017, **27**(13), 2957–2961, DOI: 10.1016/j.bmcl.2017.05.007.

31 M. S. Ayoup, D. B. Cordes, A. M. Z. Slawin and D. O'Hagan, Selectively fluorinated cyclohexane building blocks: Derivatives of carbonylated all- cis- 3-phenyl-1,2,4,5-tetrafluorocyclohexane, *Beilstein J. Org. Chem.*, 2015, **11**(1), 2671–2676, DOI: 10.3762/bjoc.11.287.

32 M. S. Ayoup, D. B. Cordes, A. M. Z. Slawin and D. O'Hagan, Total Synthesis of a Reported Fluorometabolite from Streptomyces sp. TC1 Indicates an Incorrect Assignment. The Isolated Compound Did Not Contain Fluorine, *J. Nat. Prod.*, 2014, **77**(6), 1249–1251, DOI: 10.1021/np500260z.

33 V. P. Cirillo, Mechanism of glucose transport across the yeast cell membrane, *J. Bacteriol.*, 1962, **84**(3), 485–491, DOI: 10.1128/jb.84.3.485-491.1962.

34 M. Khan, R. Ahmad, G. Rehman, *et al.*, Synthesis of Pyridinyl-benzo[d]imidazole/Pyridinyl-benzo[d]thiazole Derivatives and their Yeast Glucose Uptake Activity In Vitro, *Lett. Drug Des. Discovery*, 2019, **16**(9), 984–993, DOI: 10.2174/1570180815666181004102209.

35 L. Sim, R. Quezada-Calvillo, E. E. Sterchi, B. L. Nichols and D. R. Rose, Human Intestinal Maltase–Glucoamylase: Crystal Structure of the N-Terminal Catalytic Subunit and Basis of Inhibition and Substrate Specificity, *J. Mol. Biol.*, 2008, **375**(3), 782–792, DOI: 10.1016/j.jmb.2007.10.069.

36 C. Li, A. Begum, S. Numao, K. H. Park, S. G. Withers and G. D. Brayer, Acarbose Rearrangement Mechanism Implied by the Kinetic and Structural Analysis of Human Pancreatic α-Amylase in Complex with Analogues and Their Elongated Counterparts, *Biochemistry*, 2005, **44**(9), 3347–3357, DOI: 10.1021/bi048334e.

37 Molecular Operating Environment (MOE), *2020.09 Chemical Computing Group ULC, 1010 Sherbooke St. West*, Suite #910, Montreal, QC, Canada, H3A 2R7, 2022.

38 C. A. Lipinski, Lead- and drug-like compounds: the rule-of-five revolution, *Drug Discovery Today: Technol.*, 2004, **1**(4), 337–341.

39 T. Matsui, C. Yoshimoto, K. Osajima, T. Oki and Y. Osajima, Vitro Survey of α -Glucosidase Inhibitory Food Components, *Biosci., Biotechnol., Biochem.*, 1996, **60**(12), 2019–2022, DOI: 10.1271/bbb.60.2019.

40 K. Lalitha and V. k. Kumar, In vitro study on α-amylase inhibitory activity of an Ayurvedic medicinal plant, Anacyclus pyrethrum DC root, *Indian J. Pharmacol.*, 2014, **46**(3), 350, DOI: 10.4103/0253-7613.132204.